Loss of chloride channel ClC-5 impairs endocytosis by defective trafficking of megalin and cubilin in kidney proximal tubules

Erik I. Christensen*†, Olivier Devuyst†‡, Geneviève Dom§, Rikke Nielsen*, Patrick Van Der Smissen§, Pierre Verroust¶, Michèle Leruth§, William B. Guggino‖, and Pierre J. Courtoy§**

*Institute of Anatomy, Department of Cell Biology, University of Aarhus, DK-8000 Aarhus C, Denmark; ‡Division of Nephrology, Medical School, and §Christian de Duve Institute of Cellular Pathology, Cell Unit, Université Catholique de Louvain, B-1200 Brussels, Belgium; ¶Institut National de la Santé et de la Recherche Médicale, U538, Centre Hospitalo-Universitaire Saint Antoine, F-75012 Paris, France; and ‖Departments of Physiology and Medicine, The Johns Hopkins University School of Medicine, Baltimore, MD 21205

Communicated by Christian de Duve, Christian de Duve Institute of Cellular Pathology, Brussels, Belgium, May 13, 2003 (received for review December 19, 2002)

Loss of the renal endosome-associated chloride channel, ClC-5, in Dent's disease and knockout (KO) mice strongly inhibits endocytosis of filtered proteins by kidney proximal tubular cells (PTC). The underlying mechanism remains unknown. We therefore tested whether this endocytic failure could primarily reflect a loss of reabsorption by the multiligand receptors, megalin, and cubilin, caused by a trafficking defect. Impaired protein endocytosis in PTC of ClC-5 KO mice was demonstrated by (*i*) a major decreased uptake of injected ^{125}I-β_2-microglobulin, but not of the fluid-phase tracer, FITC-dextran, (*ii*) reduced labeling of endosomes by injected peroxidase and for the endogenous megalin/cubilin ligands, vitamin D- and retinol-binding proteins, and (*iii*) urinary appearance of low-molecular-weight proteins and the selective cubilin ligand, transferrin. Contrasting with preserved mRNA levels, megalin and cubilin abundance was significantly decreased in kidney extracts of KO mice. Percoll gradients resolving early and late endosomes (Rab5a, Rab7), brush border (villin, aminopeptidase M), and a dense peak comprising lysosomes (acid hydrolases) showed a disappearance of the brush border component for megalin and cubilin in KO mice. Quantitative ultrastructural immunogold labeling confirmed the overall decrease of megalin and cubilin in PTC and their selective loss at the brush border. In contrast, total contents of the rate-limiting endocytic catalysts, Rab5a and Rab7, were unaffected. Thus, impaired protein endocytosis caused by invalidation of ClC-5 primarily reflects a trafficking defect of megalin and cubilin in PTC.

A major function of kidney proximal tubular cells (PTC) is reabsorption and processing of plasma proteins that have escaped into the glomerular filtrate, including β_2-microglobulin (β_2M), Clara cell secretory protein, vitamin D-binding protein (DBP), and retinol-binding protein (RBP). These low-molecular-weight proteins (LMWPs) are reabsorbed by endocytosis via the multiligand tandem receptors, megalin and/or cubilin, that are abundantly expressed at the brush border of PTC (1); filtered transferrin is selectively reabsorbed by cubilin (2). Megalin, originally purified as the major autoantigen in an experimental nephritis model (3), is the largest member of the low-density lipoprotein receptor family (4). Cubilin, originally identified as the intrinsic factor cobalamin receptor (5), lacks a cytoplasmic domain and is internalized via interaction with megalin (6). Congenital or acquired diseases of PTC, collectively called Fanconi syndromes, all are characterized by LMW proteinuria (7). This defect is reproduced in megalin knockout (KO) mice and cubilin-defective dogs (8, 9).

Whereas endocytic uptake and transfer to lysosomes are catalyzed by Rab5 (10) and Rab7 (11), respectively, progression along the endocytic apparatus to lysosomes depends on endosomal acidification. The latter is achieved by the vacuolar electrogenic H^+-ATPase coupled to a chloride conductance (12). The voltage-gated chloride channel, ClC-5 (13), is almost exclusively expressed in kidney PTC and intercalated cells and is localized in endosomes (14, 15). Both inactivating mutations of ClC-5 in Dent's disease (16, 17) and *Clcn5* deletion in KO mice lead to severe LMW proteinuria because of defective endocytic uptake in PTC (18, 19). This defect has been attributed to impaired endosomal acidification (18–20). However, drugs abrogating vacuolar acidification do not affect the rate of endocytic uptake (21, 22), but inhibit recycling (23) or arrest transfer to lysosomes (21, 24–26). We therefore looked for a more specific alteration along the endocytic pathway in Dent's disease. Because of their importance in reabsorption of LMWP, we specifically asked whether defective protein endocytosis in PTC of ClC-5 KO mice could be more directly explained by a lack of megalin and cubilin at the brush border.

To this aim, we first extensively characterized the endocytic defect and found that ligands of both megalin and cubilin were affected. Next, we saw a decrease in total kidney content of megalin and cubilin but not of their mRNA. Finally, analytical subcellular fractionation and quantitative immunogold labeling both revealed a selective disappearance of megalin and cubilin at the brush border of PTC. We conclude that defective protein endocytosis linked to ClC-5 inactivation is caused by a major and selective loss of megalin and cubilin at the brush border, reflecting a trafficking defect in PTC.

Materials and Methods

Animals. Experiments were conducted on male, age-matched WT (*Clcn5*$^{+/Y}$) or KO (*Clcn5*$^{-/Y}$) adult mice generated by targeted deletion of exon VI of *Clcn5* (19). Studies were carried out in accordance with National Institutes of Health regulations for the care and use of laboratory animals.

Tracer Injection and Urine Collection. Human β_2M (Sigma) was radiolabeled with iodobeads (≈1,000 cpm/ng; >95% trichloroacetic acid-precipitable), and 620 ng/g of body weight was injected i.v. in the orbital plexus. Alternatively, mice received 2.5 mg of FITC-dextran i.v. (40 kDa, Sigma). At the indicated times, mice were anesthetized by i.p. injection of Rompun (Bayer, Brussels) and Anesketin (Eurovet, Brussels). After *in situ* kidney exsanguination, kidneys and liver were excised and total radioactivity was measured in homogenates (see below). Horseradish peroxidase (HRP) cytochemistry was performed as described

Abbreviations: β_2M, ^{125}I-β_2-microglobulin; DBP, vitamin D-binding protein; HRP, horseradish peroxidase; KO, knockout; LMWP, low-molecular-weight protein; PTC, proximal tubular cells; RBP, retinol-binding protein.

†E.I.C. and O.D. contributed equally to this work.

**To whom correspondence should be addressed. E-mail: courtoy@cell.ucl.ac.be.

www.pnas.org/cgi/doi/10.1073/pnas.1432873100

(19). Urine was collected at 4°C on Complete protease inhibitors added every 2 h (Roche Molecular Biochemicals).

Northern Blotting and Quantitative RT-PCR. Digoxigenin-labeled RNA probes for megalin, cubilin, and γ-actin were produced by RT-PCR using reported primers (4, 6, 27). Probes were localized in the rat sequence from base pairs 13762 to 14141 (GenBank accession no. L34049), 8463 to 8996 (GenBank accession no. AF022247), and 180 to 529 (GenBank accession no. X52815), respectively. The identity of PCR products was confirmed by sequencing. Total RNA (15 μg) was separated on 1% agarose-2% formaldehyde gels, transferred onto nylon membrane, washed, and cross-linked by UV. After prehybridization at 68°C, membranes were incubated for 20 h at 68°C in the presence of 20–24 μg of megalin or cubilin or 8 μg of γ-actin probe. Blots were washed, revealed by antidigoxigenin antibodies, and quantified by using the Fluor-S MultiImager system (Bio-Rad). The intensity of megalin and cubilin bands was normalized to that of actin bands. Quantitative RT-PCR was performed by the co-amplification of dilution series of an internal standard (28) that contained the same primer binding sites as the target sequence and an intervening spacer sequence, which differ by only 50–100 bp from the target. The amounts of amplified target and internal standard were quantified by the Fluor-S MultiImager system.

Western Blotting. The following antibodies were used for Western blotting: LMWP (DAKO), transferrin (DAKO), villin (29), aminopeptidase M (Santa Cruz Biotechnology), megalin (30), cubilin (31), Rab5a (Santa Cruz Biotechnology), Rab7 (32), Rab4b (gift of M. Zerial, Max Plank Institute, Dresden, Germany), cathepsin B (Santa Cruz Biotechnology), and cathepsin D (Santa Cruz Biotechnology). They were revealed by secondary anti-rabbit (BioSource International, Camarillo, CA), anti-sheep (Sigma), or anti-goat (Santa Cruz Biotechnology) secondary antibodies, followed by enhanced chemiluminescence. Western blots were quantified by using Scion (Frederick, MD) IMAGE 4.0.2.

Subcellular Fractionation. For analytical subcellular fractionation, excised kidneys were minced in 0.25 M sucrose, 3 mM imidazole buffer, pH 7.4, containing Complete protease inhibitors and homogenized in a Potter-Elvehjem tissue homogenizer (Thomas Scientific, Swedesboro, NJ). A low-speed "nuclear" fraction was pelletted at 700 × *g* for 10 min and extracted twice by resuspension sedimentation; pooled postnuclear supernatants were further sedimented at 100,000 × *g* for 60 min in a 50Ti fixed-angle rotor (Beckman, Palo Alto, CA). This high-speed pellet was resuspended in 1 ml of homogenization buffer, mixed with 7 ml of 16.08% (vol/vol) Percoll (ref. 33; average final density: 1.048 g/ml), layered over a 250-μl Percoll cushion, and centrifuged at 60,000 × *g* for 30 min in a 50Ti rotor into a self-generating gradient, after which 10 fractions of ≈750 μl each, excluding the packed cushion, were collected from the bottom. Each fraction was analyzed for density (refractometry), β-hexosaminidase activity (34), and content of the indicated antigens (Western blotting).

Immunolocalization. For immunofluorescence on semithin frozen sections, kidneys were fixed by immersion in 2% formaldehyde, 0.1 M sodium cacodylate buffer, pH 7.2, and processed as described (35) by using 1:50,000 anti-megalin, 1:1,000 anti-cubilin, 1:500 anti-DBP (DAKO), and 1:2,000 anti-RBP (DAKO) primary antibodies. For ultrastructural immunogold labeling, kidneys were fixed by retrograde perfusion through the aorta and processed as described (35) by using 1:200,000 anti-megalin or 1:10,000 anticubilin antibodies at 4°C overnight, followed (for megalin) by 1 h of incubation with rabbit anti-sheep serum (1:20,000), then with 10-nm goat anti-rabbit gold particles (1:50; Biocell Laboratories). Control sections were incubated with secondary antibodies alone or with nonspecific sheep or rabbit serum.

For morphometry, random fields of the apical cytoplasm of PTC were selected at low magnification and recorded at high magnification. In each micrograph, gold particles were attributed either to microvilli or apical vesicles and tubules, and these numbers were divided by the analyzed sectioned surface.

Statistical Analysis. Biochemical values are means ± SE and significance of differences was evaluated by one-side paired Student's *t* test. Morphometric data were analyzed by the Kolmogorov–Smirnov or the Wilcoxon signed rank test, as appropriate.

Results

Because renal phenotype resulting from a single gene inactivation may be influenced by the genetic background (36), we first characterized the endocytic deficit in our ClC-5 KO mice strain (19). Fig. 1*A* shows that, after 7 min, 22.9 ± 3.7% of i.v.-injected β_2M was retained by the kidney of WT mice vs. 3.0 ± 0.2% in KO littermates ($n = 4$; $P < 0.001$); and after 60 min, 5.3 ± 0.9% and 2.9 ± 0.2%, respectively ($P < 0.05$). Hence, whereas the tracer was rapidly degraded in WT mice, degradation was inhibited in KO mice. Liver uptake was comparable in WT and KO mice (not significant). In contrast to β_2M, kidney uptake of FITC-dextran was not affected in our strain (1.5 ± 0.2% of injected dose after 1 h in WT, vs. 1.9 ± 0.2% in KO; $n = 4$; not significant).

The deficit of LMWP endocytic uptake and trafficking in PTC from ClC-5 KO mice was further demonstrated by HRP cytochemistry that allows one to identify by light and electron microscopy accessible endocytic compartments, including lysosomes (37). At 7 min after injection to WT mice (Fig. 1*B*), HRP decorated both the brush border and multiple apical dots in PTC corresponding to apical vesicles and tubules (19). At 1 h after injection (Fig. 1*C*), staining at the brush border declined and the tracer was detected in larger endosomes and lysosomes. Whereas KO mice showed no obvious ultrastructural alteration in PTC (Fig. 1*C*), staining at 7 min after HRP injection was essentially restricted to the brush border (Fig. 1*B*); at 1 h, many fewer apical vesicles and tubules were labeled than in WT kidney, and lysosomal staining was exceptional (Fig. 1*C*). In contrast, the staining pattern in Kupffer and liver endothelial cells was identical in KO and WT mice (data not shown).

This PTC defect in KO mice was reflected by extensive urinary excretion of LMWP, identifying defective receptor-mediated endocytosis by megalin, and of transferrin, pointing to a concomitant deficit of cubilin (Fig. 1*D*). In an interesting contrast, the amount of megalin, but not of cubilin, shed in the urine was greatly decreased in KO mice (≈3-fold). In both WT and KO mice, daily urinary excretion of megalin and cubilin corresponded to <1% of total kidney content. KO mice also showed selective urinary excretion of the PTC lysosomal enzyme, cathepsin B (Fig. 1*D*).

Renal expression of megalin and cubilin in ClC-5 KO mice revealed no deficit at the mRNA level, as shown by Northern blotting (megalin, 121 ± 36% of control; cubilin, 122 ± 42%; $n = 3$; not significant) and RT-PCR. In contrast, the content of both receptors, as shown by Western blotting, was reduced in total kidney extracts (Table 1). This was confirmed by immunofluorescence in two littermate pairs that also showed defective uptake of the endogenous ligands DBP and RBP (Fig. 2).

Quantitative Western blotting analysis was extended to several other markers of the brush border, endosomes, and lysosomes in the kidneys (Table 1). In contrast to megalin and cubilin, there was no loss of the brush border cytoskeletal marker, villin, as could be predicted by the integrity of this structure by electron microscopy (Fig. 1*C*; see also Fig. 4), nor of aminopeptidase M,

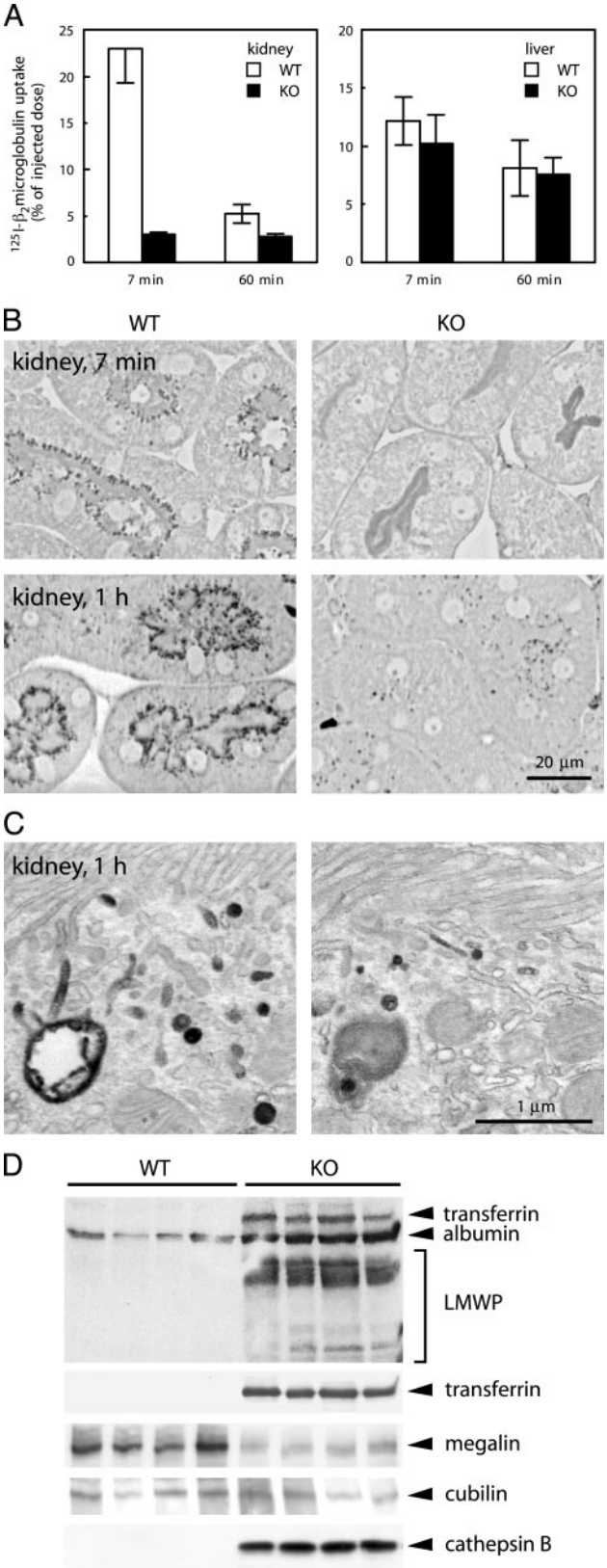

Fig. 1. Selective impairment of protein endocytosis in PTC from ClC-5 KO mice. (*A*) Quantitation of the uptake deficit. At 7 min or 1 h after i.v. injection of ^{125}I-β_2M to control (WT) and ClC-5 KO mice (KO), radioactivity was measured in bleached kidneys and liver ($n = 4$). (*B* and *C*) Visualization of the apical endocytic apparatus by light (*B*) and ultrastructural (*C*) cytochemistry at 7 or 60 min after HRP injection. (*B Upper*) At 7 min, the reaction product stains the brush border (gray signal next to the collapsed lumen) in WT and KO, whereas multiple apical dots immediately thereunder are seen only in WT. (*B Lower* and *C*) At 1 h after injection to WT mice, HRP mostly labels small endocytic vesicles and dense apical recycling tubules and includes larger structures, whereas labeling is greatly reduced in KO mice. (*D*) Urine analysis by Western blotting. Urinary excretion of LMWPs, transferrin, and cathepsin B in KO mice is obvious, contrasting with decreased urinary loss of megalin and normal excretion of cubilin.

Table 1. Total content of endocytic apparatus markers in ClC-5 KO mice

	n	% of controls	*P*
LMWP receptors			
Megalin	5	72 ± 5	<0.01
Cubilin	5	26 ± 8	<0.001
Brush border			
Villin	5	95 ± 16	NS
Aminopeptidase M	4	126 ± 57	NS
Endosomes			
Rab5a	5	92 ± 9	NS
Rab7	4	105 ± 18	NS
Rab4b	5	89 ± 18	NS
Lysosomes			
β-Hexosaminidase (activity)	5	36 ± 4	<0.001
Cathepsin B (mature form)	4	53 ± 11	<0.01
Cathepsin D (mature form)	5	93 ± 8	NS

Total kidney extracts of four or five littermate pairs were analyzed for the indicated constituents by Western blotting or enzymatic activity (β-hexosaminidase). Values were normalized per mg of tissue protein, and specific activities in KO mice were expressed by reference to WT littermates. NS, not significant.

an apical marker enzyme of PTC. The content of the endocytic catalysts, Rab5a, Rab7, and Rab4b, generally used as markers of early, late, and recycling endosomes, respectively, was also unaffected by ClC-5 inactivation. Thus, among membrane markers, the deficit of cubilin and megalin was selective and compatible with a receptor trafficking defect. This suggestion could also account for the observed decrease in ClC-5 KO kidneys of the two lysosomal enzymes, β-hexosaminidase and cathepsin B, that are abundantly expressed in PTC (Table 1). In contrast, there was no difference in kidneys for cathepsin D, mostly abundant in cortical collecting ducts (38), nor for β-hexosaminidase in liver (104 ± 10% of control; $n = 5$; not significant).

The possibility of a trafficking defect in kidneys of ClC-5 KO mice was further addressed by subcellular fractionation in Percoll gradients (Fig. 3), which clearly resolved a low-density peak (fractions 2–3), including early (Rab5a) and late (Rab7) endosomal markers; an intermediate density peak (fractions 6–9), including the brush border markers, villin and aminopeptidase M; and a bottom peak enriched in lysosomes (cathepsins B and D) and recycling endosomes (Rab4b; data not shown). There was no difference in these density distributions between WT and ClC-5 KO mice, allowing for a direct comparison (Fig. 3). The density distribution of cubilin was clearly bimodal in WT kidneys, comprising an endosomal peak and a brush border peak; the latter was abrogated in KO mice. Surprisingly, the density distribution of megalin analyzed in the very same fractions as for cubilin was not bimodal in WT kidneys, reminiscent of the fact that megalin does not fully colocalize with cubilin by immunofluorescence (39). As for cubilin, megalin in KO mice was depleted from brush border fractions and enriched in endosomal fractions (Fig. 3). This fractionation analysis thus strongly indicated that both residual pools of megalin and cubilin were selectively depleted from the brush border upon ClC-5 inactivation. Interestingly, there was a similar shift of β-hexosamini-

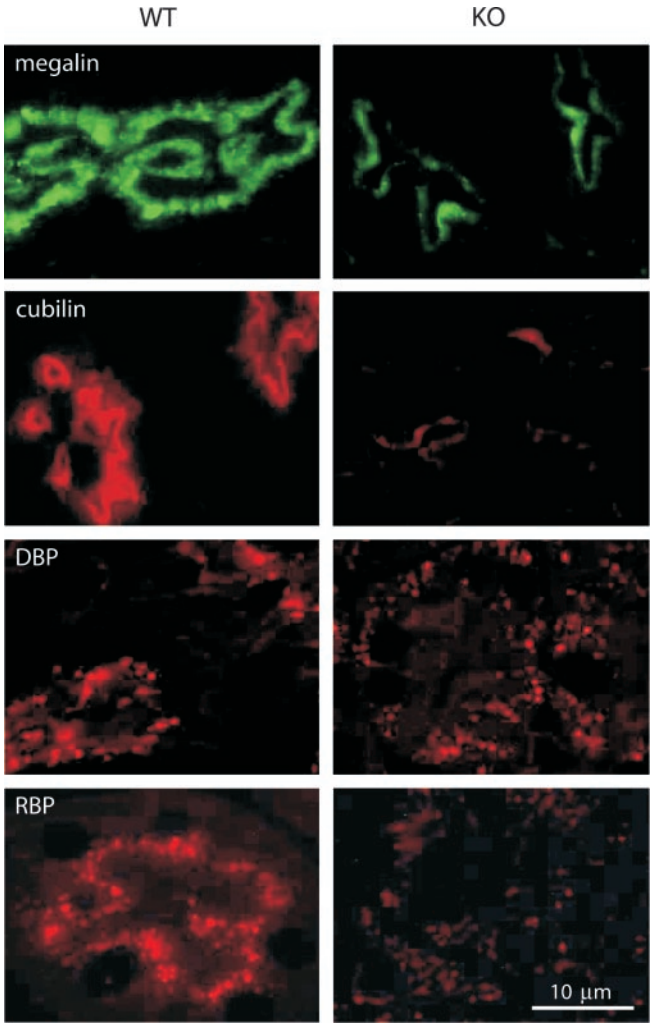

Fig. 2. Immunofluorescence. The strong apical signal, seen for megalin and cubilin in WT proximal tubules, is markedly decreased in KO mice. Likewise, the granular staining for reabsorbed endogenous DBP and RBP is strongly reduced in ClC-5 KO kidneys.

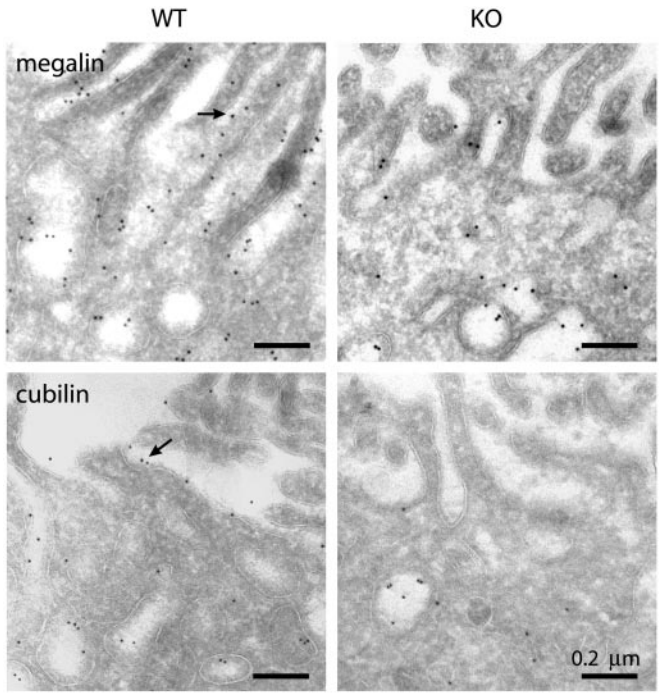

Fig. 4. Immunogold labeling of megalin and cubilin on ultrathin frozen sections of renal cortices. Arrows indicate labeling at brush border, which is much reduced in KO as compared with WT mice.

dase and β_2M, from a predominant dense peak in WT mice to a more bimodal distribution in KO mouse kidneys, pointing to an associated endocytic trafficking defect of soluble proteins normally destined to lysosomes.

Finally, immunogold labeling revealed in KO mice a systematic decrease of megalin and cubilin in apical endosomes and recycling tubules and their almost complete disappearance at the brush border (Fig. 4). Morphometry confirmed an overall decrease of megalin and cubilin in KO mice (≈3-fold), with a preferential loss (≈6-fold) for both antigens at the brush border (Table 2).

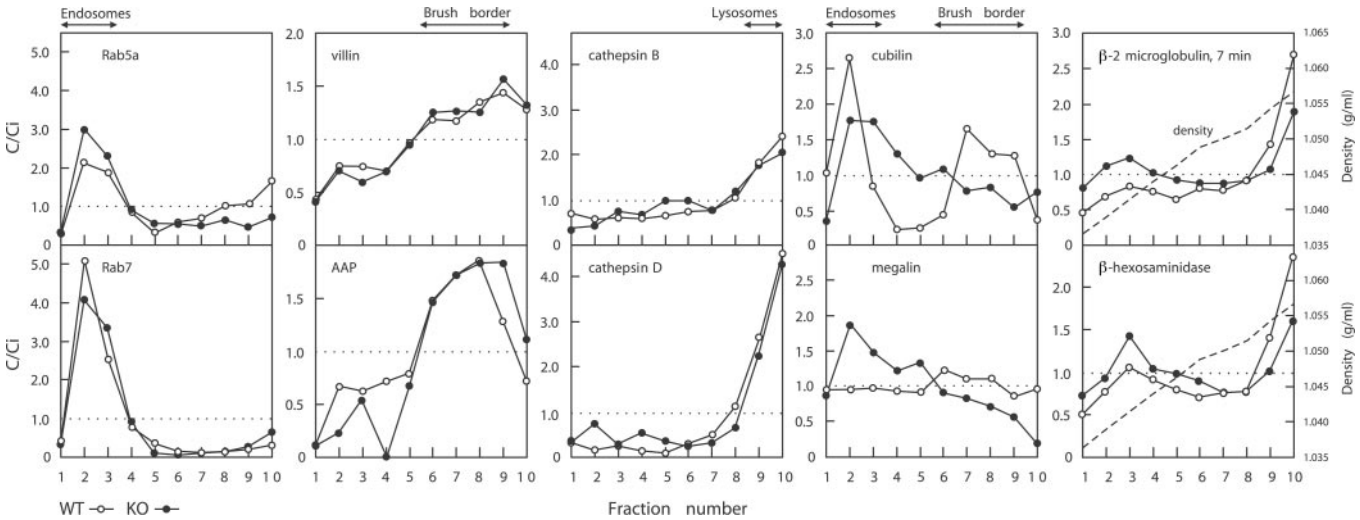

Fig. 3. Subcellular fractionation in Percoll gradients. Average density in seven gradients is indicated by a broken line. Dotted lines indicate initial concentration. Distributions after centrifugation are presented as C/Ci indices, where values >1 reflect organelle enrichment and values <1 reflect organelle depletion. Typical distributions representative of at least three fractionation analyses for each constituent are shown for control (WT, ○) and corresponding KO littermates (●). Distributions of ^{125}I-β_2-M were comparable after 7 min and 1 h.

Table 2. Quantitation of immunogold labeling

Section analyzed	WT	KO
Megalin	(n = 12; 67 μm^2)	(n = 20; 116 μm^2)
Apical cytoplasm	83.6 ± 27.0	28.3 ± 20.1
Apical microvilli	18.4 ± 19.2	3.3 ± 5.0
Apical vesicles and tubules	126.1 ± 33.6	64.9 ± 32.0
Cubilin	(n = 34; 194 μm^2)	(n = 32; 202 μm^2)
Apical cytoplasm	13.4 ± 4.4	4.0 ± 2.8
Apical microvilli	7.3 ± 4.0	1.2 ± 1.6
Apical vesicles and tubules	18.0 ± 8.0	6.3 ± 3.7

Numbers of analyzed micrographs and total analyzed surface per sample are indicated in parentheses. Labeling intensity values are expressed as means ± SD of gold particles per μm^2 of analyzed sections in apical cytoplasm of PTC, further subdivided in microvilli and apical vesicles/tubules. Background was <0.03 particles per μm^2. Differences in labeling intensity between WT and KO mice, and in each case between microvilli and vesicles/tubules, were all significant ($P < 0.01$).

Discussion

This article shows that impaired endocytosis of filtered proteins secondary to ClC-5 inactivation primarily reflects the disappearance of megalin and cubilin at the brush border of PTC. These alterations contrast with the absence of detectable ultrastructural anomaly, deficit of endocytic catalysts, and inhibition of accumulation of a fluid-phase trace in the analyzed mouse strain. It results from a decrease of the total pool of both receptors, aggravated by a trafficking defect.

The failure of apical protein endocytosis in PTC of ClC-5 KO mice was evidenced by (*i*) a 7-fold lower uptake of the megalin ligand, β_2M, (*ii*) a major decrease of intracellular labeling in PTC for HRP and the endogenous megalin ligands DBP and RBP, and (*iii*) a strong urinary excretion of the LMWP ligands of megalin and the selective ligands of cubilin, transferrin (2), and Clara cell secretory protein (19). Impaired protein endocytosis, similar to that of patients with Dent's disease (16, 17), is specific for the kidney, because there was no detectable change in liver uptake of β_2M and HRP.

Despite considerable interest in apical endocytosis (40, 41), the mechanisms underlying the deficit of protein reabsorption by PTC upon ClC-5 inactivation remain unknown. Because ClC-5 codistributes with endosomes (14, 15), impaired endosomal acidification caused by the lack of the chloride conductance necessary to neutralize the electrogenic vacuolar H^+-ATPase in PTC endosomes was suggested as a straightforward explanation for apical endocytic failure (18–20). This notion is supported by indirect evidence, based on decreased ATP-dependent fluorescence quenching of low-density vesicles loaded *in vitro* by acridine orange. The significance of the latter observation remains, however, unclear, because residual quenching in vesicles of ClC-5 KO mice still showed chloride dependence (42). Furthermore, coated vesicles, i.e., the primary endocytic vesicles, are not acidified (43) and pharmacological inhibition of endosomal acidification does not affect the primary endocytic rate (21, 22).

A second possibility for a failure of apical endocytosis caused by the lack of ClC-5 would be a general structural defect of the endocytic apparatus or impaired recruitment on primary endocytic pits of a rate-limiting endocytic catalyst such as Rab5a, or a component of their coat (44), that would be retained on less acidified endosomes. However, in contrast to megalin KO mice (8), ClC-5 KO mice showed no detectable ultrastructural anomaly in PTC (see Fig. 1*C*), as we recently reported in Dent's disease (45). In particular, there was no obvious qualitative difference in apical immunolabeling for clathrin (preliminary observations). Furthermore, we found that accumulation of the nonproteinaceous fluid-phase tracer, FITC-dextran, was not reduced and that neither the content nor the density distribution of Rab5a were affected upon ClC-5 inactivation.

The third mechanism we considered was a defective overall expression of the endocytic receptors, megalin and cubilin, in ClC-5 KO mouse kidneys. A partial decrease of megalin has been suggested (18) and was precisely quantified by the present study. Moreover, the deficit of the tandem receptor, cubilin, demonstrated in this study, was ≈3-fold that of megalin. Decreased expression was not caused by a defect at the mRNA level, indicating accelerated receptor loss. The negligible urinary excretion of both receptors in WT and KO mice strongly argues against accelerated shedding and further points to an intracellular defect. However, the overall decrease of megalin is too moderate to provide a sufficient explanation for a failure of LMWP endocytosis, because endocytic receptors are expressed in vast excess and because mice heterozygous for megalin gene inactivation do not exhibit LMW proteinuria (8).

The lack of a satisfactory explanation by the three above mechanisms led us to investigate the possibility that failure of apical protein endocytosis by PTC in ClC-5 KO mice would be caused mostly by redistribution of the residual content of megalin and cubilin, from the brush border to intracellular endocytic organelles. This hypothesis was directly demonstrated by subcellular fractionation and quantitative immunogold labeling, both revealing a much more severe loss of the two receptors at the brush border of PTC. This observation might account for the reduced shedding of megalin in the urine, as also reported in Dent's disease (46).

Besides defective endocytic uptake, a further trafficking defect in PTC of ClC-5 mouse kidneys is impaired progression toward lysosomes. This is indicated by (*i*) the strong inhibition of the degradation of internalized β_2M and the reduced accessibility of lysosomes to HRP, (*ii*) the similar alteration in the density distribution of injected β_2M and endogenous hexosaminidase, (*iii*) the specific decrease of the PTC lysosomal enzymes, β-hexosaminidase and cathepsin B, and (*iv*) the selective loss of cathepsin B in the urine. Impaired vacuolar acidification is known to prevent progression toward lysosomes, thereby rerouting endocytic tracers (21) and newly synthesized lysosomal enzymes (47) to the recycling pathway. Acidification is indeed necessary for the recruitment on endosomes of COP coat proteins (26) and the small GTPase, Arf6, and its exchange factor, ARNO (48).

We therefore suggest that intracellular trafficking of selected membrane proteins and their ligands in PTC of ClC-5 KO mice is affected at three levels: (*i*) a slower apical internalization, as also indicated in the other ClC-5 KO mice strain by a slower redistribution from the brush border to endocytic vesicles of the sodium/phosphate exchanger, NaPi-2, and the sodium/proton exchanger, NHE3, in response to parathormone (18); (*ii*) a more severe slowing down of the recycling of megalin and cubilin to the brush border that would explain their preferential retention in endosomes; and (*iii*) impaired transfer of endocytic tracers to lysosomes. Thus, ClC-5 inactivation primarily inhibits apical protein endocytosis in PTC by causing a trafficking defect of megalin and cubilin, in the absence of ultrastructural alterations of the apical endocytic apparatus and apparent deficit in rate-limiting endocytic catalysts. It remains to be clarified to what extent ClC-5 inactivation impairs endosomal acidification, and if/how the latter explains the selective loss of megalin and cubilin at the brush border.

E.I.C. and P.C. dedicate this work to Dr. Werner Straus, who introduced HRP as a tracer in cell biology, first identified kidney lysosomes, and discovered endosomes. We thank I. B. Kristoffersen, Y. Cnops, Y. Marchand, P. K. Nielsen, H. Sidelmann, and T. Lac for excellent assistance. We are grateful for the gift of valuable antibodies from Drs. S. Robine (villin) and M. Zerial (Rab4b and Rab7). This study was funded in Denmark by the Medical Research Council and Novo Nordic Foundation; in Belgium by the Forton Foundation, Fonds National de la Recherche Scientifique, Inter-University Attraction Poles, and Concerted Research Actions, and in the United States by National Institutes of Health Grant DK32793.

1. Christensen, E. I. & Birn, H. (2002) *Nat. Rev. Mol. Cell Biol.* **3,** 256–266.
2. Kozyraki, R., Fyfe, J., Verroust, P. J., Jacobsen, C., Dautry-Varsat, A., Gburek, J., Willnow, T. E., Christensen, E. I. & Moestrup, S. K. (2001) *Proc. Natl. Acad. Sci. USA* **98,** 12491–12496.
3. Kerjaschki, D. & Farquhar, M. G. (1982) *Proc. Natl. Acad. Sci. USA* **79,** 5557–5581.
4. Saito, A., Pietromonaco, S., Loo, A. K. & Farquhar, M. G. (1994) *Proc. Natl. Acad. Sci. USA* **91,** 9725–9729.
5. Seetharam, B., Christensen, E. I., Moestrup, S. K., Hammond, T. G. & Verroust, P. J. (1997) *J. Clin. Invest.* **99,** 2317–2322.
6. Moestrup, S. K., Kozyraki, R., Kristiansen, M., Kaysen, J. H., Rasmussen, H. H., Brault, D., Pontillon, F., Goda, F. O., Christensen, E. I., Hammond, T. G. & Verroust, P. J. (1998) *J. Biol. Chem.* **273,** 5235–5242.
7. Van t'Hoff, W. (2000) *Arch. Dis. Child.* **83,** 189–191.
8. Nykjaer, A., Dragun, D., Walther, D., Vorum, H., Jacobsen, C., Herz, J., Melsen, F., Christensen, E. I. & Willnow, T. E. (1999) *Cell* **96,** 507–515.
9. Nykjaer, A., Fyfe, J. C., Kozyraki, R., Leheste, J.-R., Jacobsen, C., Nielsen, M. S., Verroust, P. J., Aminoff, M., de la Chapelle, A., Moestrup, S. K., *et al.* (2001) *Proc. Natl. Acad. Sci. USA* **98,** 13895–13900.
10. Bucci, C., Parton, R. G., Mather, I. H., Stunnenberg, H., Simons, K., Hoflack, B. & Zerial, M. (1992) *Cell* **70,** 715–728.
11. Vitelli, R., Santillo, M., Lattero, D., Chiariello, M., Bifulco, M., Bruni, C. B. & Bucci, C. (1997) *J. Biol. Chem.* **272,** 4391–4397.
12. Mellman, I., Fuchs, R. & Helenius, A. (1986) *Annu. Rev. Biochem.* **55,** 663–700.
13. Jentsch, T. J., Stein, V., Weinreich, F. & Zdebik, A. A. (2002) *Physiol. Rev.* **82,** 503–568.
14. Günther, W., Lüchow, A., Cluzeaud, F., Vandewalle, A. & Jentsch, T. J. (1998) *Proc. Natl. Acad. Sci. USA* **95,** 8075–8080.
15. Devuyst, O., Christie, P. T., Courtoy, P. J., Beauwens, R. & Thakker, R. V. (1999) *Hum. Mol. Genet.* **8,** 247–257.
16. Lloyd, S. E., Pearce, S. H., Fisher, S. E., Steinmeyer, K., Schwappach, B., Scheinman, S. J., Harding, B., Bolino, A., Devoto, M., Goodyer, P., *et al.* (1996) *Nature* **379,** 445–449.
17. Scheinman, S. J., Guay-Woodford, L. M., Thakker, R. V. & Waronck, D. G. (1999) *N. Engl. J. Med.* **340,** 1177–1187.
18. Piwon, N., Gunther, W., Schwake, M., Bosl, M. R. & Jentsch, T. J. (2000) *Nature* **408,** 369–373.
19. Wang, S. S., Devuyst, O., Courtoy, P. J., Wang, X. T., Wang, H., Wang, Y., Thakker, R. V., Guggino, S. & Guggino, W. B. (2000) *Hum. Mol. Genet.* **9,** 2937–2945.
20. Marshansky, V., Ausiello, D. A. & Brown, D. (2002) *Curr. Opin. Nephrol. Hypertens.* **11,** 527–537.
21. Cupers, P., Veithen, A., Hoekstra, D., Baudhuin, P. & Courtoy, P. J. (1997) *Biochem. Biophys. Res. Commun.* **236,** 661–664.
22. Tyteca, D., Van Der Smissen, P., Mettlen, M., Van Bambeke, F., Tulkens, P. M., Mingeot-Leclercq, M.-P. & Courtoy, P. J. (2002) *Exp. Cell Res.* **281,** 86–100.
23. Basu, S. K., Goldstein, J. L., Anderson, R. G. & Brown, M. S. (1981) *Cell* **24,** 493–502.
24. Limet, J. N., Quintart, J., Schneider, Y.-J. & Courtoy, P. J. (1985) *Eur. J. Biochem.* **146,** 539–548.
25. van Deurs, B., Holm, P. K. & Sandvig, K. (1996) *Eur. J. Cell Biol.* **69,** 343–350.
26. Aniento, F., Gu, F., Parton, R. G. & Gruenberg, J. (1996) *J. Cell Biol.* **133,** 29–41.
27. Brown, C. W., McHugh, K. M. & Lessard, J. L. (1990) *Nucleic Acids Res.* **18,** 5312.
28. Bor, M. V., Sorensen, B. S., Rammer, P. & Nexo, E. (1998) *Clin. Chem.* **44,** 1154–1160.
29. Robine, S., Huet, C., Moll, R., Sahuquillo-Merino, C., Coudrier, E., Zweibaum, A. & Louvard, D. (1985) *Proc. Natl. Acad. Sci. USA* **82,** 8488–8492.
30. Moestrup, S. K., Nielsen, S., Andreasen, P., Jorgensen, K. E., Nykjaer, A., Roigaard, H., Gliemann, J. & Christensen, E. I. (1993) *J. Biol. Chem.* **268,** 16564–16570.
31. Sahali, D., Mulliez, N., Chatelet, F., Laurent-Winter, C., Citadelle, D., Sabourin, J. C., Roux, C., Ronco, P. & Verroust, P. J. (1993) *Am. J. Pathol.* **142,** 1654–1667.
32. Chavrier, P., Parton, R. G., Hauri, H. P., Simons, K. & Zerial, M. (1990) *Cell* **62,** 317–329.
33. Dickson, R. B., Beguinot, L., Hanover, J. A., Richert, N. D., Willingham, M. C. & Pastan, I. (1983) *Proc. Natl. Acad. Sci. USA* **80,** 5335–5339.
34. Leaback, D. H. & Walker, P. G. (1961) *Biochem. J.* **78,** 151–156.
35. Christensen, E. I., Nielsen, S., Moestrup, S. K., Borre, C., Maunsbach, A. B., de Heer, E., Ronco, P., Hammond, T. G. & Verroust, P. (1995) *Eur. J. Cell Biol.* **66,** 349–364.
36. Devuyst, O. & Guggino, W. B. (2002) *Am. J. Physiol.* **283,** F1176–F1191.
37. Straus, W. (1962) *J. Cell Biol.* **12,** 231–246.
38. Yokota, S., Tsuji, H. & Kato, K. (1985) *J. Histochem. Cytochem.* **33,** 191–200.
39. Verroust, P. J. & Christensen, E. I. (2002) *Nephrol. Dial. Transplant.* **17,** 1867–1871.
40. Mostov, K. E., Verges, M. & Altschuler, Y. (2000) *Curr. Opin. Cell Biol.* **12,** 483–490.
41. Sandvig, K. & Van Deurs, B. (2002) *Annu. Rev. Cell Dev. Biol.* **18,** 1–24.
42. Günther, W., Piwon, N. & Jentsch, T. J. (2003) *Pflügers Arch. Eur. J. Physiol.* **445,** 456–462.
43. Fuchs, R., Ellinger, A., Pavelka, M., Mellman, I. & Klapper, H. (1994) *Proc. Natl. Acad. Sci. USA* **91,** 4811–4815.
44. Marsh, M. & McMahon, H. T. (1999) *Science* **285,** 215–220.
45. Moulin, P., Igarashi, T., Van Der Smissen, P., Cosyns, J.-P., Verroust, P., Thakker, R. V., Scheinman, S. J., Courtoy, P. J. & Devuyst, O. (2003) *Kidney Int.* **63,** 1285–1295.
46. Norden, A. G. W., Lapsley, M., Igarashi, T., Kelleher, C. L., Lee, P. J., Matsuyama, T., Scheinman, S. J., Shiraga, H., Sundin, D. P., Thakker, R. V., *et al.* (2002) *J. Am. Soc. Nephrol.* **13,** 125–133.
47. Gonzalez-Noriega, A., Grubb, J. H., Talkad, V. & Sly, W. S. (1980) *J. Cell Biol.* **85,** 839–852.
48. Maranda, B., Brown, D., Bourgoin, S., Casanova, J. E., Vinay, P., Ausiello, D. A. & Marshansky, V. (2001) *J. Biol. Chem.* **276,** 18540–18550.